Tetrahedron 67 (2011) 1091–1095

Contents lists available at ScienceDirect

Tetrahedron

journal homepage: www.elsevier.com/locate/tet

A FRET approach for luminescence sensing Cr^{3+} in aqueous solution and living cells through functionalizing glutathione and glucose moieties

Xiaoyue Hu, Xiaolin Zhang, Guangjie He, Cheng He, Chunying Duan *

State Key Laboratory of Fine Chemicals, Dalian University of Technology, Dalian 116012, China

ARTICLE INFO

Article history:
Received 20 September 2010
Received in revised form 2 December 2010
Accepted 10 December 2010
Available online 16 December 2010

Keywords:
Chemosensor
Cr^{3+}
Glucose tolerance factors
FRET

ABSTRACT

A simple FRET-based approach to ratiometric fluorescence sensing of Cr^{3+} in aqueous solution using glutathione and glucose as building blocks was achieved, inspired to the binding motifs of Cr^{3+} in glucose tolerance factors (GTF). Selectivity and competition experiments showed that this system featured high sensitivity (detection limit $\leq$0.1 ppm) and excellent selectivity over other metal ions in buffer solution. Confocal fluorescence microscopy experiments had established the utility of the approach in monitoring Cr^{3+} within living cells.

1. Introduction

Trivalent chromium, Cr(III), is an essential component of a balanced human and animal diet,[1] in amounts of 50–200 μg per day. The deficiency of chromium would cause disturbances in the glucose levels and lipid metabolism, and lead to a variety of disease, including diabetes and cardiovascular disease.[2,3] At the mean time, chromium is an environmental pollutant and its build-up due to various industrial and agricultural activities is a matter of concern.[4] Thus, there is an urgent need to develop chemical sensors that are capable of detecting the presence of chromium ions in environmental and biological samples in aqueous media.

On the other hand, fluorescent chemosensor is an active field of molecular chemistry.[5,6] The reigning paradigm for the fluorescent chemosensor discovery has facilitated the bioimaging Ca^{2+},[7] Zn^{2+},[8] Hg^{2+},[9] Cu^{2+},[10] and Pb^{2+}[11] ions in living cells. However, the development of new chemosensors for intracellular and extracellular Cr^{3+} imaging remains extremely challenging, owing to the lack of special selective binding events and the fluorescence quenching of paramagnetic Cr^{3+}.[12] And of these Cr^{3+} probes reported,[13] several display drawbacks in terms of actual applicability, such as lack of water solubility or the cross-sensitivities toward other metal ions.

Since the mechanism by which Cr^{3+} affects human metabolism is based on modulation of the action of insulin through glucose tolerance factors (GTF), the binding motifs around Cr^{3+} observed in the available structure of the GTF inspires the development of artificial sensor molecules.[14] Our interest in this area concentrates on Cr^{3+} chemosensor that possesses a relative approach to a ratiometric fluorescence response using glutathione and glucose as building blocks (Scheme 1). It is expected that the coordination of Cr^{3+} will lead to efficient Förster resonance energy transfer (FRET)[15] from the coumarin energy donor of the glutathione-relative receptor (**CG1**) to the ring-opened rhodamine moiety of the glucose-relative receptor (**RG1**).[16] The mixed system possibly affords the simultaneous recording of two emission intensities at different wavelengths and has the potential to increase the selectivity and sensitivity and to eliminate most of the possible variability.[17]

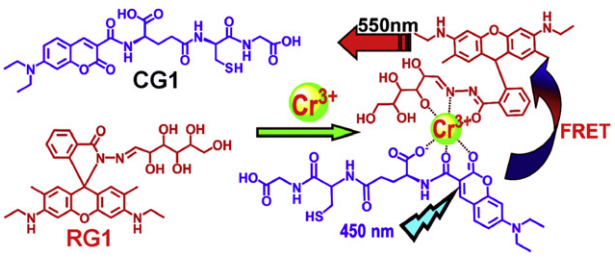

Scheme 1. Structure of glutathione-relative (**CG1**) and glucose-relative (**RG1**) parts of the Cr^{3+} receptors, showing the proposed bonding model relative to the bonding motifs of Cr^{3+} in GTF.

* Corresponding author. Tel.: +86 411 8370 2355; fax: +86 411 3989 3830; e-mail address: cyduan@dlut.edu.cn (C. Duan).

0040-4020/$ – see front matter © 2010 Elsevier Ltd. All rights reserved.
doi:10.1016/j.tet.2010.12.026

2. Results and discussion

2.1. Synthesis and spectral properties of CG1

Glutathione-based receptor **CG1** was synthesized from the reaction of succinimidyl ester of 7-diethylamino-coumarin-3-carboxylic acid and glutathione in DMF for 48 h. It exhibited biocompatibility and excellent water solubility. **CG1** displayed a characteristic coumarin absorption band[18] in the visible region centered at 425 nm (Fig. 1). Upon addition of $CrCl_3$ to the solution of **CG1**, the absorbance at 425 nm decreased gradually and then remained constant after adding approximately 1.3 mM Cr^{3+}. The presence of isosbestic points reflected the existence of only one intermediate complex. Fitting of the titration curve revealed a 2:1 stoichiometry of the **CG1**–Cr^{3+} complexation species with the association constant of 3.94×10^6 M^{-2}.[19]

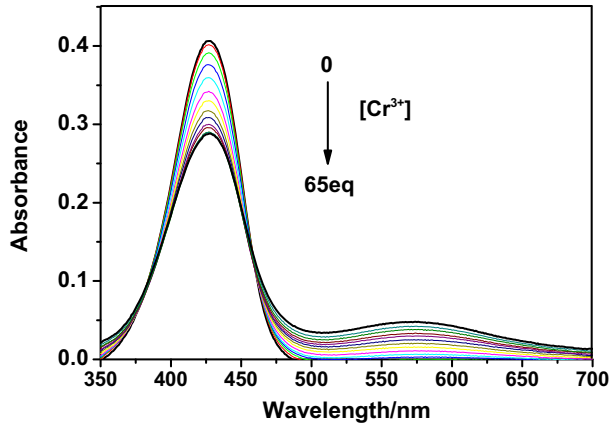

Fig. 1. Absorption spectra of **CG1** (20 μM) for Cr^{3+} ions (0–65 equiv) in NaAc–HAc buffer solution (20 mM, pH=6.0). Each spectrum was acquired 4 min after Cr^{3+} addition.

Free receptor **CG1** exhibited a strong emission at 475 nm (Fig. 2), assignable to the coumarin unit (Φ_f=0.012)[18] upon excitation at 450 nm. The addition of Cr^{3+} ions, caused fluorescence quenching and showed a steady and smooth decrease until a plateau was reached (Φ_f=0.005). Fitting of the titration curve also suggested a 2:1 stoichiometry **CG1**–Cr^{3+} complexation species. Under the same conditions no fluorescence changes of **CG1** (20 μM in NaAc–HAc buffer solution, pH=6.0) were observed in the presence of alkali and alkali earth metal ions; however, by the addition of transition metal ions, the fluorescence decreased to varying degree. Especially the addition of 50 equiv of Fe^{3+} or Cu^{2+} caused about fivefold fluorescence decrease of **CG1**.

2.2. Synthesis and spectral properties of RG1

Glucose-based receptor **RG1** was prepared by the reaction of glucose unit and Rhodamine-6G hydrazide in a methanol/toluene mixed solution. It also had excellent water solubility and favorable biocompatibility and had been used as a mercury sensor in natural water.[20] Free **RG1** solution exhibited almost no absorption peak in the visible wavelength range in NaAc–HAc buffer solution (20 mM, pH=6.0). Upon addition of Cr^{3+}, a absorption band centered at 535 nm, assignable to the delocalized xanthene moiety of the rhodamine group[21] appeared and developed gradually (Fig. 3). The individual profile of the absorbance at 535 nm demonstrated a 2:1 stoichiometric complex for **RG1**–Cr^{3+}, with the association constant calculated as 3.96×10^5 M^{-2}.[19]

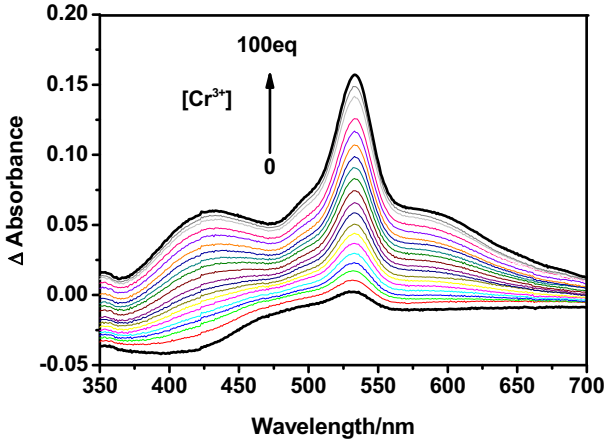

Fig. 3. Different absorption spectra of **RG1** (20 μM) for Cr^{3+} ions (0–100 equiv) in NaAc–HAc buffer solution (20 mM, pH=6.0). Each spectrum was acquired 4 min after Cr^{3+} addition.

RG1 in buffer solution exhibited a weak emission (Φ_f=0.15) at about 555 nm (excitation at 490 nm, Fig. 4). By addition of Cr^{3+}, the emission band increased significantly (Φ_f=0.28), demonstrating the formation of the xanthene tautomer of the rhodamine group.[21] The luminescence titration profile also suggested a 2:1 stoichiometry of the **RG1**–Cr^{3+} complexation species. **RG1** exhibited very little

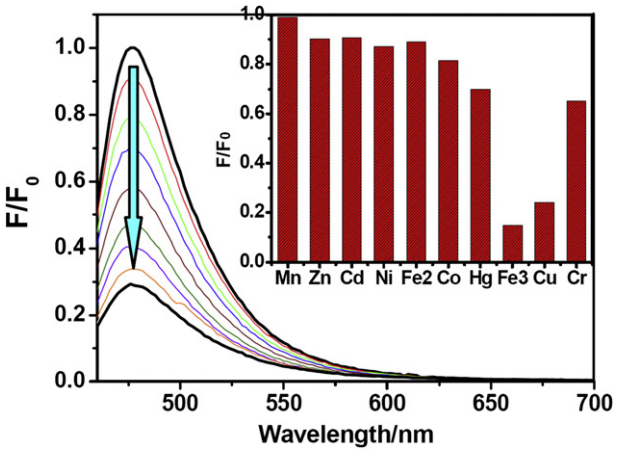

Fig. 2. Fluorescence responses of **CG1** (20 μM) in NaAc–HAc buffer solution (20 mM, pH=6.0) upon addition of Cr^{3+} ions (0–2 mM). Inset: the fluorescence responses for several metal ions (1 mM), fluorescence responses were recorded at 475 nm, excitation at 450 nm.

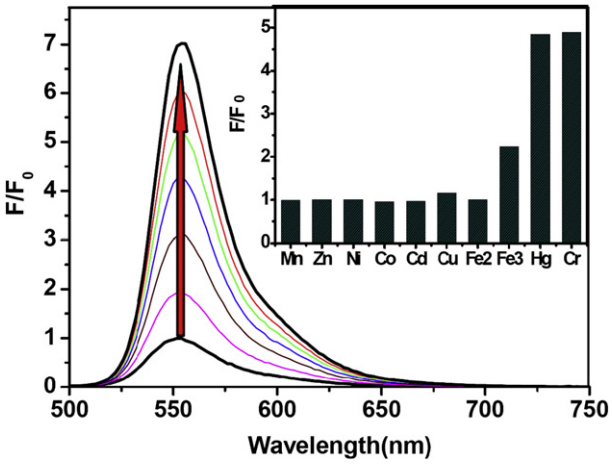

Fig. 4. Fluorescence responses of **RG1** (20 μM) upon addition of Cr^{3+} ions (0–2 mM) in NaAc–HAc buffer solution (20 mM, pH=6.0). Inset: the fluorescence responses for several metal ions (1 mM), fluorescence intensities were recorded at 555 nm, excitation at 490 nm.

fluorescence enhancement at 555 nm upon addition of 50 equiv of various metal ions mentioned; however, the addition of Hg^{2+} or Fe^{3+} also resulted in a prominent fluorescence enhancement.[20]

2.3. Spectral properties of CG1+RG1

Since the use of **CG1** or **RG1** as the Cr^{3+} probes was restricted by their poor selectivity, we combined the two compounds into one system for selectively sensing Cr^{3+}, which inspired to the binding motifs of Cr^{3+} in GTF. As the probes **CG1** and **RG1** had the different binding affinities for Cr^{3+}, the ratio of the two probes in the mixture and other experimental conditions were optimized by maintaining a total concentration of 0.2 mM in a NaAc–HAc buffer solution (0.1 M, pH=6.0). The inflection point at about 0.33 suggested the 1:2 mol-ratio between **CG1** and **RG1** is the most proper one for luminescent detection Cr^{3+} in aqueous solutions (Fig. 5 left).

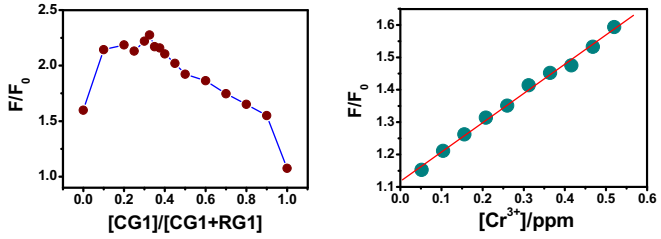

Fig. 5. Left: the fluorescence intensity versus the [**CG1**]/[**CG1**+**RG1**] with a total concentration ([**CG1**]+[**RG1**]) maintained at 0.2 mM in NaAc–HAc buffer solution (0.1 M, pH=6.0); right: fluorescence intensity changes of **CG1**–**RG1** (1:2) (1 μM) in NaAc–HAc buffer solution (20 mM, pH=6.0) upon additions of Cr^{3+} ions (1–10 μM). Excitation was provided at 450 nm, and the emission intensities were integrated at 555 nm.

The optimized solution of **CG1** (20 μM) and **RG1** (40 μM) in a NaAc–HAc buffer solution (20 mM, pH=6.0) exhibited an absorption band centered at 425 nm. The addition of Cr^{3+} caused an obvious absorbance decrease at 425 nm (Fig. 6). At the same time, a new peak at 535 nm appeared and developed significantly. This gave a visual color change from yellow to pink (inset of Fig. 6).

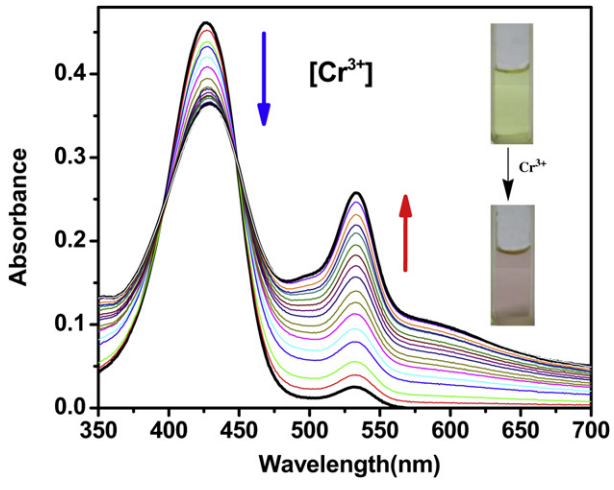

Fig. 6. Absorption spectra of **CG1** (20 μM) and **RG1** (40 μM) in NaAc–HAc buffer solution (20 mM, pH=6.0) in the presence of different amounts of Cr^{3+} (0–2 mM). Each spectrum was acquired 4 min after Cr^{3+} addition. Inset: change in color of the above solution before and after addition of Cr^{3+}.

The above mentioned solution exhibited a strong emission band centered at about 475 nm (excited at 450 nm). Upon gradual addition of Cr^{3+} ions, the intensity of the emission band centered at 475 nm decreased gradually and that of a new fluorescent band centered at 555 nm increased gradually (Fig. 7). As a result, an

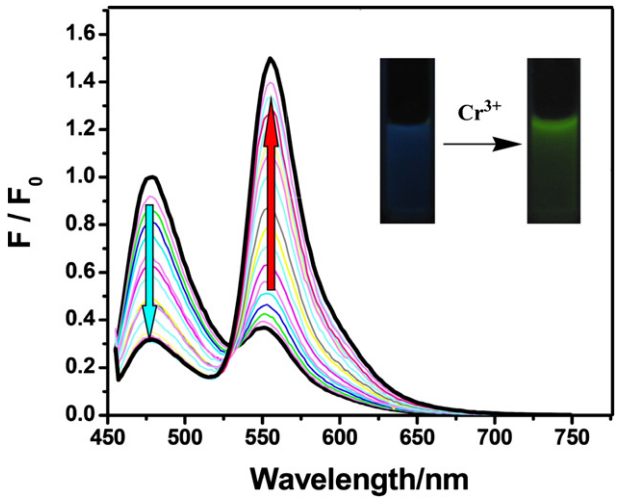

Fig. 7. Fluorescence spectra of the combined **CG1** (20 μM) and **RG1** (40 μM) upon the addition of Cr^{3+} in 20 mM NaAc–HAc buffer solution (pH=6.0), with the excitation at 450 nm. Insert: change in fluorescence of the above solution before and after addition of Cr^{3+}.

obvious change in fluorescent color from blue to green was observed (inset of Fig. 7). In the presence of 2 mM Cr^{3+}, the ratio of final and the initial emission intensities at 555 nm (F/F_0) was up to 5. This observation was consistent with increased FRET from coumarin (donor) to the open colored form of rhodamine (acceptor) as shown in Scheme 1. Time-dependent fluorescence measurements exhibited that the fluorescence lifetimes of **CG1** and **RG1** were 2.807 ns and 3.972 ns, respectively. In the **CG1**+**RG1**+**Cr^{3+}** system, the fluorescence lifetimes were 2.52 ns (**CG1**) and 3.978 ns (**RG1**), respectively. The considerably shorter lifetime (0.287 ns) of the emission at 475 nm of **CG1** suggested the possibility of energy transfer from the coumarin moiety to the Rhodamine-6G moiety.

Fluorescence measurements also exhibited an excellent selectivity toward Cr^{3+} over metal ions. As depicted in Fig. 8, no significant spectral changes were observed in the presence of alkali-, alkaline-earth metals, such as Na^{+}, K^{+}, Mg^{2+}, Ca^{2+}, and the first-row transition metals Mn^{2+}, Fe^{2+}, Fe^{3+}, Co^{2+}, Ni^{2+}, Cu^{2+}, and Zn^{2+}, respectively. Even the presence of Cd^{2+} and Pb^{2+} could not bring any obvious fluorescence change.

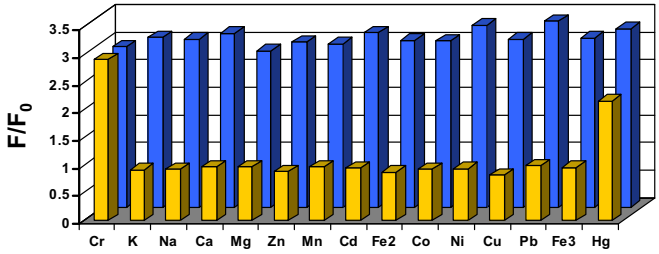

Fig. 8. Fluorescence responses of solution containing **CG1** (20 μM) and **RG1** (40 μM) to various metal ions in NaAc–HAc buffer solution (20 mM pH=6.0). The yellow bars represent the integrated fluorescence in the presence of various metal ions (1 mM). The blue bars represent the fluorescence upon the addition of Cr^{3+} (1 mM) to the above mentioned solution (except for Cr^{3+} solution). The fluorescence was recorded at 555 nm, excitation at 450 nm.

The addition of Hg^{2+} gave a twofold enhancement of emission, which was weaker than that caused by the addition of Cr^{3+}. From the spectral titrations of these receptors, it could be found that the stoichiometry of the complexation species is 1:1 for Hg(II), indicative the difficulty stands on the co-existence of two receptors within one Hg^{2+} complexation species. Thus the FRET response of the **CG1**–**RG1** system is hardly observed in case of Hg^{2+}. The

presence of the above mentioned metal ions and even the Hg^{2+} did not influence the fluorescence responses of Cr^{3+} in aqueous solution, indicating the good selectivity toward Cr^{3+} over other competitive cations. Furthermore, under the experimental conditions, the fluorescence intensities of the solution containing **CG1** (20 μM) and **RG1** (40 μM) in a NaAc–HAc buffer solution (20 mM, pH=6.0) were nearly proportional to the amount of Cr^{3+} (0–0.5 ppm, Fig. 5 right). The parts per million level detection limit for Cr^{3+} suggested the possible application in toxicology and environmental sciences.

2.4. Cell imaging

Importantly, the approach exhibited the practical applicability as a Cr^{3+} probe in the fluorescence imaging of living cells. HeLa cells were incubated for 15 min with 20 μM **CG1** and 40 μM **RG1** at room temperature to allow the probe to permeate into the cells. Under selective excitation with longer-wavelength light at 488 nm, cells gave no intracellular fluorescence (Fig. 9A). When the cells stained with solution containing the probes were incubated with $CrCl_3$ (1.2 mM) in normal saline for another 15 min and washed, a significant green fluorescence intensity in live cells was observed (Fig. 9B). Bright-field measurement confirmed that the cells after treatment with the probes solution and Cr^{3+} were viable throughout the imaging experiments (Fig. 9C). As shown in Fig. 9D, the overlay of fluorescence and bright-field images revealed that the fluorescence signals were localized in the perinuclear region of the cytosol, thus indicating the subcellular distribution of Cr^{3+}. Unfortunately, no obvious FRET process was observed, which probably due to the complicated environment in cell.

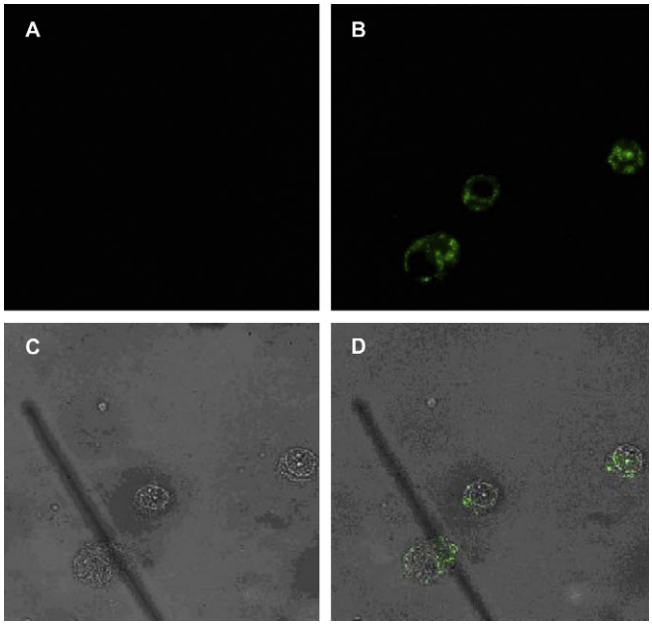

Fig. 9. Confocal fluorescence images of HeLa cells. (A) Cells incubated with 20 μM **CG1** and 40 μM **RG1** in normal saline for 15 min. (B) Cells incubated with the above mentioned solution for 15 min, then washed three times, and further stained with 1.2 mM Cr^{3+} for 15 min. (C) Bright-field image of cells showed in panel (B). The overlay image of (B) and (C) was shown in (D) (λ_{ex}=488 nm).

3. Conclusion

In summary, we have investigated the optical responses of the two receptors **CG1** and **RG1**, having glutathione and glucose as building blocks inspired to the binding motifs of Cr^{3+} in glucose tolerance factors. Both of them displayed high sensitivity but poor selectivity toward Cr^{3+} in aqueous solution. However, combining the two receptors as one system could detect Cr^{3+} in aqueous buffer with excellent selectivity and sensitivity (detection limit ≤0.1 ppm). We anticipate that the new approach provided here will help in the design of fluorescent chemosensors for the Cr^{3+} ion and of benefit to biomedical researchers for studying the bioactivity of Cr^{3+} in biological systems.

4. Experimental

4.1. Instruments and reagents

All the solvents and reagents were of analytic grade and used without further purification. The salts solutions of metal ions were $NaClO_4 \cdot H_2O$, KNO_3, $Ca(NO_3)_2$, $Mg(ClO_4)_2$, $Zn(ClO_4)_2 \cdot 6H_2O$, $Pb(ClO_4)_2 \cdot 3H_2O$, $Mn(ClO_4)_2 \cdot 6H_2O$, $Co(ClO_4)_2 \cdot 6H_2O$, $Ni(ClO_4)_2 \cdot 6H_2O$, $Cd(ClO_4)_2 \cdot 6H_2O$, $CuCl_2$, $Hg(ClO_4)_2 \cdot 3H_2O$, $FeCl_2 \cdot 4H_2O$, $FeCl_3 \cdot 6H_2O$, and $CrCl_3 \cdot 6H_2O$. NaAc–HAc buffer solutions (20 mM and 50 mM, pH=6.0) were prepared in water.

^1H NMR and ^{13}C NMR were taken on Varian Inova-400 spectrometer with TMS as an internal standard and $CDCl_3$/DMSO-d_6 as solvent. Mass spectrometric data were obtained with a LCQ-Tof MS spectrometry. IR spectra were recorded using KBr pellets on a Vector 22 Bruker spectrophotometer in the 4000–400 cm^{-1} regions. Fluorescence spectra were determined with FS920 luminescence spectrometer (Edinburgh instruments). UV–vis spectra were recorded on a Lambda35 UV–vis spectrophotometer. All pH measurements were made with a Model PHS-3C meter.

4.2. General procedures of spectra detection

Stock solutions of the metal ions (20 mM) were prepared in deionized buffer aqueous. A stock solution of **CG1** (1 mM) was prepared in DMF and a stock solution of **RG1** (1 mM) was prepared in ethanol. The solutions of **CG1** and **RG1** were then diluted to 20 μM, respectively, with NaAc–HAc buffer solutions (20 mM and 50 mM, pH=6.0). And the mixed solution of **CG1** and **RG1** was diluted to 20 μM (**CG1**) in a ratio of 1:2 with NaAc–HAc buffer solutions (20 mM and 50 mM, pH=6.0). In titration experiments, each time a 2 mL NaAc–HAc buffer solution (20 mM, pH=6.0) of **CG1** or **RG1** or **CG1**–**RG1** (1:2) (20 μM) was filled in a quartz optical cell of 1 cm optical path length, and the Cr^{3+} stock solution was added into the quartz optical cell gradually by using a micro-pippet. Spectral data were recorded at 4 min after the addition. In selectivity experiments, the test samples were prepared by placing 50 equiv amounts of metal ion stock into 2 mL NaAc–HAc buffer solution (50 mM, pH=6.0 for Fe^{3+}; 20 mM, pH=6.0 for the other metal ions) of **CG1** or **RG1** or **CG1**–**RG1** (1:2) (20 μM). In competition experiments, 50 equiv amount of metal ion stock was added after that the NaAc–HAc buffer solution (50 mM, pH=6.0 for Fe^{3+}; 20 mM, pH=6.0 for the other metal ions) of **CG1** or **RG1** or **CG1**–**RG1** (1:2) (20 μM) with 50 equiv amount of Cr^{3+} was stirred for 3 h. For fluorescence measurements, excitation was provided at 450 nm, and emission was collected from 460 to 750 nm. F_0 represented the initial peak value of the fluorescence emission before the addition of Cr^{3+}. All the spectroscopic measurements were performed at least in triplicate and averaged.

The binding constant was calculated from the absorption-titration curve according to the equation.

$$\mathrm{Log}((A - A\mathrm{min})/(A\mathrm{max} - A)) = \log k + n\log[c]$$

Where A is the absorption of **CG1** (**RG1**) at 425 nm (535 nm) upon addition of different amounts of Cr^{3+}. [c] stands for the concentration of Cr^{3+}.

4.3. Quantum yield measurement

Fluorescence quantum yield was determined using optically matching solutions of Rhodamine-6G (Φ_f=0.94 in ethanol) as standards at an excitation wavelength of 500 nm and the quantum yield is calculated using Eq. (1).[22]

$$\phi_{unk} = \phi_{std}\frac{(I_{unk}/A_{unk})}{(I_{std}/A_{std})}\left(\frac{\eta_{unk}}{\eta_{std}}\right)^2 \quad (1)$$

Where Φ_{unk} and Φ_{std} are the radiative quantum yields of the sample and standard, I_{unk} and I_{std} are the integrated emission intensities of the corrected spectra for the sample and standard, A_{unk} and A_{std} are the absorbance of the sample and standard at the excitation wavelength (500 nm for Rhodamine-6G, 450 nm for **CG1** and 490 nm for **RG1**).

4.4. Cell incubation and imaging

HeLa cells were cultured in 1640 supplemented with 10% FCS (Invitrogen) or DMEM culture medium+10% FBS+1% PS+1% Glutmax. Cells were seeded on 18 mm glass coverslips. After 12 h, HeLa cells were incubated with 20 μM **CG1** and 40 μM **RG1** (in the culture medium containing 0.5% DMSO) for 15 min at room temperature and then washed with normal saline (pH=7) three times. After incubating with 1.2 mM $CrCl_3$ for another 15 min at room temperature, the HeLa cells were rinsed with normal saline (pH=7) three times again. The glass coverslips were attached to slide before imaging.

Confocal fluorescence imaging was performed with a Leica TCS-SP2 laser scanning microscopy and a 20× oil-immersion objective lens. Excitation wavelength of laser was 488 nm. Emission was centered at 550±25 nm (single channel).

4.5. Synthesis

CG1. To a solution of glutathione (1.4736 g, 4.8 mmol) and *N*-ethyldiisopropylamine (1 mL) in DMF (6 mL), succinimidyl ester of 7-diethylamino-coumarin-3-carboxylic acid[17](0.2147 g , 0.6 mmol) in DMF (30 mL) was added dropwise. The reaction was stirred at room temperature for 48 h. After filtration, the solvent was evaporated in vacuum and the residue was purified by silica gel chromatography ($CH_3COOC_2H_5$–CH_3OH=5:1, v/v) to give product as a yellow solid (0.2588 g, 78.5%). Mp: 160.6–163.2 °C. ESI-MS: *m/z* 573.2656 for [**CG1**+Na]$^+$. ^{1}H NMR (400 MHz, DMSO-d_6) δ 9.02 (t, 1H), 8.67 (s, 1H), 8.27 (d, 1H), 8.14 (d, 1H), 7.70 (d, 1H), 6.82 (d, 1H), 6.65 (s, 1H), 4.51 (t, 1H), 4.39 (t, 1H), 3.72 (d, 2H), 3.49 (q, 4H), 3.33 (s, 2H), 2.78 (s, 1H), 2.66 (s, 1H), 2.36–2.10 (m, 4H), 1.93 (s, 1H), 1.15 (t, 6H). ^{13}C NMR (400 MHz, DMSO-d_6) δ 169.97, 167.46, 161.93, 161.56, 161.15, 157.70, 152.82, 148.11, 132.01, 130.18, 129.12, 110.18, 02108.07, 96.29, 65.51, 63.13, 56.12, 44.79, 30.44, 19.11, 14.01, 12.76. IR (solid KBr pellet cm^{-1}): 3389.66(s), 3067.40(m), 2934.88(m), 1649.22(s), 1512.04(s), 1418.76(m), 1351.38(w), 1230.36(m), 1135.67(w), 1076.40(w).

Acknowledgements

We gratefully acknowledge financial support from the National Natural Science foundation of China.

Supplementary data

Supplementary data associated with this article can be found in the online version at doi:10.1016/j.tet.2010.12.026.

References and notes

1. Shanker, A. K. Mode of Action and Toxicity of Trace Elements In *Trace Elements: Nutritional Benefits, Environmental Contamination, and Health Implications*; Prasad, M. N. V., Ed.; John Wiley: Hoboken, NJ, 2008; pp 537–542.
2. McRae, R.; Bagchi, P.; Sumalekshmy, S.; Fahrni, C. J. *Chem. Rev.* **2009**, *109*, 4780–4827.
3. Anderson, R.; Chromium, R. A. *Trace Elements in Human and Animal Nutrition*; Academic: New York, NY, 1987.
4. Cervantes, C.; Campos-García, J.; Devars, S.; Gutiérrez-Corona, F.; Loza-Tavera, H.; Torres-Guzmán, J. C.; Moreno-Sánchez, R. *FEMS Microbiol. Rev.* **2001**, *25*, 335–347.
5. Desvergne, J. P.; Czarnik, A. W. *Chemosensors of Ion and Molecular Recognition, NATO ASI Series*; Kluwer Academic: Netherlands, 1997; C492.
6. de Silva, A. P.; Gunaratne, H. Q. N.; Gunnlaugsson, T.; Huxley, A. J. M.; McCoy, C. P.; Rademacher, J. T.; Rice, T. E. *Chem. Rev.* **1997**, *97*, 1515–1566.
7. (a) Arunkumar, E.; Ajayaghosh, A.; Daub, J. *J. Am. Chem. Soc.* **2005**, *127*, 3156–3164; (b) Kim, H. M.; Kim, B. R.; Hong, J. H.; Park, J. S.; Lee, K. J.; Cho, B. R. *Angew. Chem., Int. Ed.* **2007**, *46*, 7445–7448.
8. (a) Qian, F.; Zhang, C. L.; Zhang, Y. M.; He, W. J.; Gao, X.; Hu, P.; Guo, Z. J. *J. Am. Chem. Soc.* **2009**, *131*, 1460–1468; (b) Wong, B. A.; Friedle, S.; Lippard, S. J. *J. Am. Chem. Soc.* **2009**, *131*, 7142–7152.
9. Nolan, E. M.; Lippard, S. J. *Chem. Rev.* **2008**, *108*, 3443–3480.
10. (a) Liu, J.; Lu, Y. *J. Am. Chem. Soc.* **2007**, *129*, 9838–9839; (b) Jung, H. S.; Kwon, P. S.; Lee, J. W.; Kim, J.; Hong, C. S.; Kim, J. W.; Yan, S.; Lee, J. Y.; Lee, J. H.; Joo, T.; Kim, J. S. *J. Am. Chem. Soc.* **2009**, *131*, 2008–2012.
11. (a) Kwon, J. Y.; Jang, Y. J.; Lee, Y. J.; Kim, K. M.; Seo, M. S.; Nam, W.; Yoon, J. Y. *J. Am. Chem. Soc.* **2005**, *127*, 10107–10111; (b) He, Q. W.; Miller, E. W.; Wong, A. P.; Chang, C. J. *J. Am. Chem. Soc.* **2006**, *128*, 9316–9317.
12. (a) Som-Aum, W.; Threeprom, J.; Li, H. F.; Lin, J. M. *Talanta* **2007**, *71*, 2062–2068; (b) Singh, A. K.; Gupta, V. K.; Gupta, B. *Anal. Chim. Acta* **2007**, *585*, 171–178.
13. (a) Mao, J.; Wang, L. N.; Dou, W.; Tang, X. L.; Yan, Y.; Liu, W. S. *Org. Lett.* **2007**, *9*, 4567–4570; (b) Zhou, Z. G.; Yu, M. X.; Yang, H.; Huang, K. W.; Li, F. Y.; Yi, T.; Huang, C. H. *Chem. Commun.* **2008**, 3387–3389; (c) Huang, K. W.; Yang, H.; Zhou, Z. G.; Yu, M. X.; Li, F. Y.; Gao, X.; Yi, T.; Huang, C. H. *Org. Lett.* **2008**, *10*, 2557–2560.
14. (a) Mertz, W.; Schwarz, K. *Arch. Biochem. Biophys.* **1955**, *58*, 504–506; (b) Meyer, J. A.; Spence, D. M. *Metallomics* **2009**, *1*, 32–41.
15. Sapsford, K. E.; Berti, L.; Medintz, I. L. *Angew. Chem., Int. Ed.* **2006**, *45*, 4562–4588.
16. Komatsu, T.; Kikuchi, K.; Takakusa, H.; Hanaoka, K.; Ueno, T.; Kamiya, M.; Urano, Y.; Nagano, T. *J. Am. Chem. Soc.* **2006**, *128*, 15946–15947.
17. Albers, A. E.; Okreglak, V. S.; Chang, C. J. *J. Am. Chem. Soc.* **2006**, *128*, 9640–9641.
18. Lin, W. Y.; Yuan, L.; Cao, X. W.; Tan, W.; Feng, Y. M. *Eur. J. Org. Chem.* **2008**, 4981–4987.
19. Shiraishi, Y.; Sumiya, S.; Kohno, Y.; Hirai, T. *J. Org. Chem.* **2008**, *73*, 8571–8574.
20. Huang, W.; Zhou, P.; Yan, W. B.; He, C.; Xiong, L. Q.; Li, F. Y.; Duan, C. Y. *J. Environ. Monit.* **2009**, *11*, 330–335.
21. Kim, H. N.; Lee, M. H.; Kim, H. J.; Kim, J. S.; Yoon, J. Y. *Chem. Soc. Rev.* **2008**, *37*, 1465–1472.
22. Fischer, M.; Georges, J. *Chem. Phys. Lett.* **1996**, *260*, 115–118.